

Vertically Aligned Carbon Nanotubes as Pixel Detector Substrate

Vittorio Boccone*

DECTRIS Ltd., System Integration, Täfernweg 1, 5405 Baden-Dättwil, Switzerland

E-mail: vittorio.boccone@dectris.com

*10th International Workshop on Semiconductor Pixel Detectors for Particles and Imaging (Pixel2022),
12-16 December 2022
Santa Fe, New Mexico, USA*

*Speaker

1. Introduction

In Transmission Electron Microscopy (TEM) the modulation transfer function (MTF) and the detective quantum efficiency (DQE) are two of the key performance indicators for the resolution of a detector system. Higher spatial resolution is often achieved by reducing the pixel size and, at the same time, thinning down the active sensor thickness in an attempt to escape the stochastic effects ruling the evolution of the primary and secondary electron tracks in the material.

Both, the electrons directly backscattered from the active sensor and those backscattered from the material below the active sensor, contribute to the reduction of the performances by lowering the MTF and in turn the DQE. Active electronics on the pixel sensor itself also require cooling.

The reduction of the backscattering and the thermal control of semiconductor detectors operated in vacuum conditions are two common problems to face when designing high-resolution, low-background and low-noise particle detectors. It's well known that low-Z materials, such as Aluminum or Beryllium reduce the intensity of the backscattered radiation (electrons or photons) as the radiation travels deep into the media, and the fraction of the backscattered radiation is reduced, but not suppressed.

2. Vertically Aligned Carbon Nanotubes

Carbon Nano-Tubes (CNTs) possess extraordinary electrical conductivity, heat conductivity, mechanical and chemical properties. Vertically Aligned Carbon Nano-Tubes (VACNTs) in particular are one-dimensional structures (Fig. 1 left), where the different nanotubes are grown next to each other by chemical vapor deposition (CVD). VACNT layers can be grown up to a thickness of 1 mm, and have shown outstanding directionality properties in ion channeling [3], electron penetration [8], and other applications [9]. VACNTs layers are used to grant directionality in cathodes for photomultipliers [2]. VACNTs can also be used in flip-chip packaging systems [12] when they are segmented into “bumps”, as shown in Fig. 1 (right).

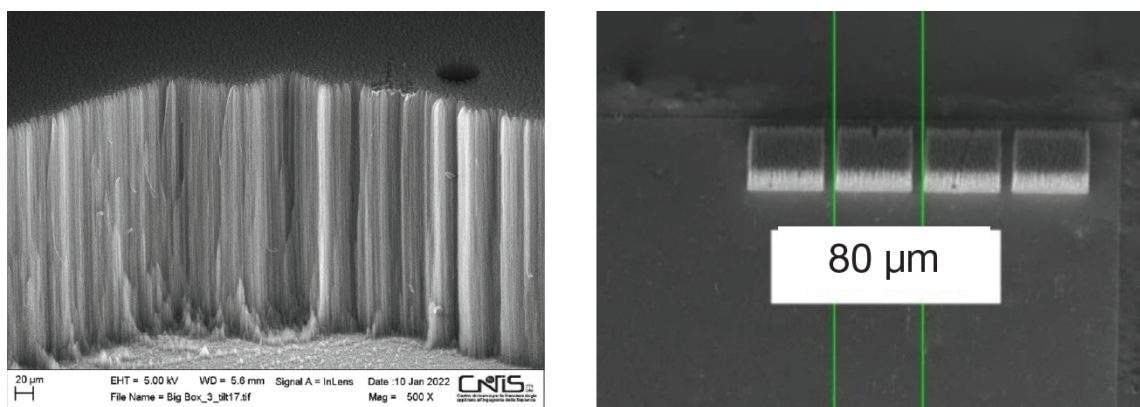


Figure 1: Examples of VACNTs structures. Left: simple VACNT forest used to grant directionality in cathodes for photomultipliers [2]. Right: segmented VACNTs “bumps” for the flip-chip packaging system [12].

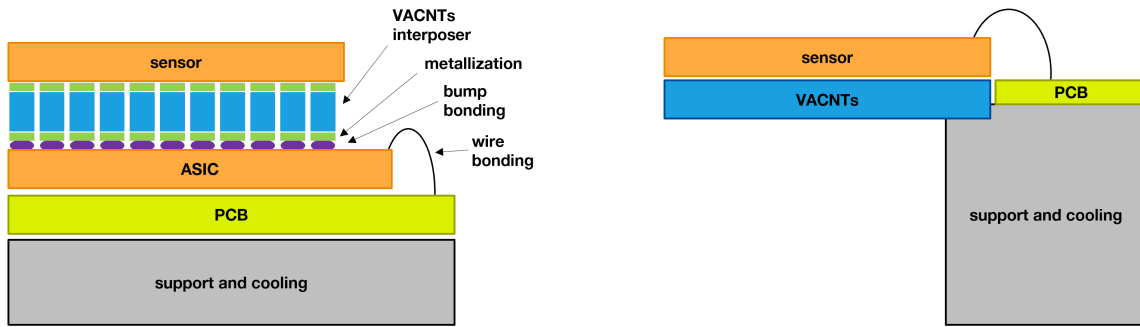


Figure 2: Possible usage of VACNTs in Hybrid Pixel Detectors (left) and in MAPS Detectors (right).

I propose in this paper the usage of VACNTs as the sensor substrate, or in the case of hybrid detectors, as a pixelated interposer between the ASIC and the active sensor. In both cases, as illustrated in Fig.2, the VACNT layer would assure an optimal heat extraction channel when coupled with an active cooling system. A decrease in the intensity of the backscattered radiation (photon and/or electrons) entering the detector from the back would be also granted by the low atomic number of carbon.

3. Simulations

The angular distribution and the energy spectrum of the backscattered radiation are not uniform. Both have an impact on the correct determination of the impact point of the original electron. In order to start exploring the possibility of using this structure as an interposer between the ASIC and the sensor, or as a detector substrate, we need to understand the characteristics of the radiation backscattered to the sensor.

3.1 Model

I simulated the interaction of a 300 keV pencil electron beam impinging on a simplified detector assembly, illustrated in Fig. 3 (left), composed by an active sensor, a 1 mm thick VACNT substrate, a 500 μm thick silicon ASIC, a 200 μm thick flex PCB, and a 5 mm thick Aluminum support. For the active sensor we considered different thicknesses and materials. The sensor configurations used for this study are summarized in Tab. 1. For this first investigations no further details (such as metallization layers, bump bonding, etc . . .) were included.

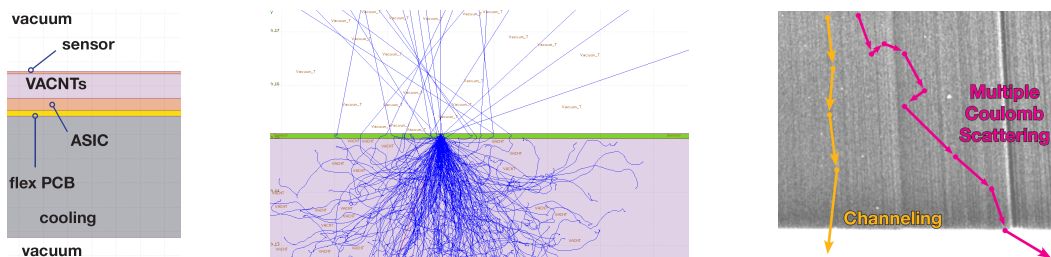


Figure 3: Left: simple simulation model. Center: tracks in the detector assembly. Right: capturing and channeling of charged particles from the VACNTs.

Material	Thickness [μm]
Si	35, 50, 100, 150, 200, 300
GaAs	10, 250
CdTe	75

Table 1: Sensor configurations used for this study.

As of today, channelling effects are not included in any of the major Monte-Carlo simulation frameworks such as Geant4 [7], Fluka [5, 6], Penelope [10], and Allpix Squared [1]. Prior works [2, 3] suggest the presence of channeling and dechanneling conditions on energy and entrance angle. Those conditions define whether or not the electron will interact with the carbon as an amorphous material or will be scattered along the aligned VACNTs instead. Channeling effects in VACNTs were not simulated, and the layer was modeled as graphite with scaled density.

The simulation including the channeling and dechanneling conditions could potentially be handled in Fluka, or Geant4. In both cases we would define a special external routine that describes the interaction of the electrons with the VACNTs structure. We could in alternative include a modified multiple Coulomb scattering formulation that takes into account the bulk effects rather than the single interaction. This modelling would need to include properties of the specific VACNT layers, multi walled VACNTs, single walled VACNTs, tree density, and more. This will be the focus of future work.

Thicker high-Z sensor configurations were included as a reference to evaluate the effects of the sensor on the backscattering of the primary radiation. The $10\ \mu\text{m}$ thin GaAs sensor configuration, which might appear at first quite exotic and unrealistic, was included to investigate what could happen if the growth of a thin GaAs sensor [11] could be coupled with the growth of VACNTs on GaAs [4]. The simulations were performed using the Fluka Monte-Carlo framework [5, 6] and, the VACNTs were approximated as an amorphous material with an adjusted material density.

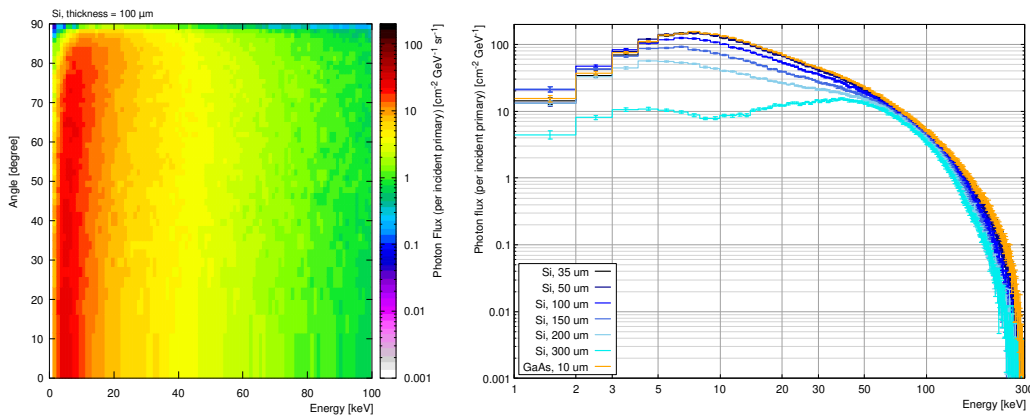


Figure 4: Distribution of the backscattered photons as a function of energy and exit angle for a silicon sensor with a thickness of $100\ \mu\text{m}$ (left) and distribution of the backscattered photons as a function of energy for different sensor configurations (right).

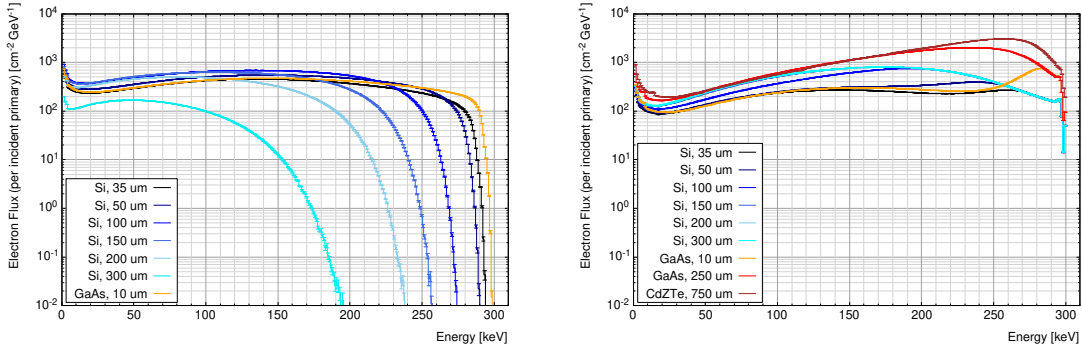


Figure 5: Spectrum of the electrons backscattered from the VACNT layer (left) and from the sensor (right).

3.2 Backscattered photons

Electron detectors are also sensitive (fully or in part) to the photon part of the backscattered radiation. Its impact is at least two orders of magnitudes lower than the backscattered electron, because of the fluence and the limited sensitivity that a thinned detector has for those energies. The angular distribution of the backscattered photons, visible in Fig. 4 (left), is typically isotropic.

Above 50 keV, the photon flux exiting from the VACNT surface decreases almost linearly with the reduction of the sensor thickness. The photons below 50 keV have a non-negligible probability to be absorbed in the sensor and contribute to the creation of a pixel cluster. This effect is particularly evident for increasing sensor thicknesses where the peak in the fluence at 5-8 keV is suppressed for thicknesses above 200–250 μm as shown in Fig. 4 (right).

3.3 Backscattered electrons

The biggest contribution to the degeneration of the resolution comes from the backscattered electrons. As before, the thicker the sensor the softer the spectrum, as can be seen from the spectrum of the electrons backscattered from the VACNT layer shown in Fig. 5 (left). The spectrum suppression for electrons is way stronger than the one for photons. In addition, the distribution of the backscattered electrons from the layer below the sensor (Fig. 6) is not anymore isotropic.

According to [3, 8] the electrons backscattered at small angles have a higher probability of being channeled than those scattered at larger angles to which the material would appear amorphous, as illustrated in Fig. 3 (right).

The role of the VACNTs layer would be to enhance the part of the spectrum at small exit angle (below 20°), and simultaneously suppress the part of the spectrum at larger exit angles (above 30°).

The DQE is also affected by the fraction of the primary beam which is directly bouncing off the sensor surface (with or without prior interaction). This effect is stronger for high-Z materials such as CdTe or CZT although, the reduction of the thickness help to minimize its effects. However, this has nothing to do with the detector substrate, it's worth mentioning that sensor thicknesses above 150 μm will only have limited benefits from the mitigation of the backscattering effects introduced by the VACNTs.

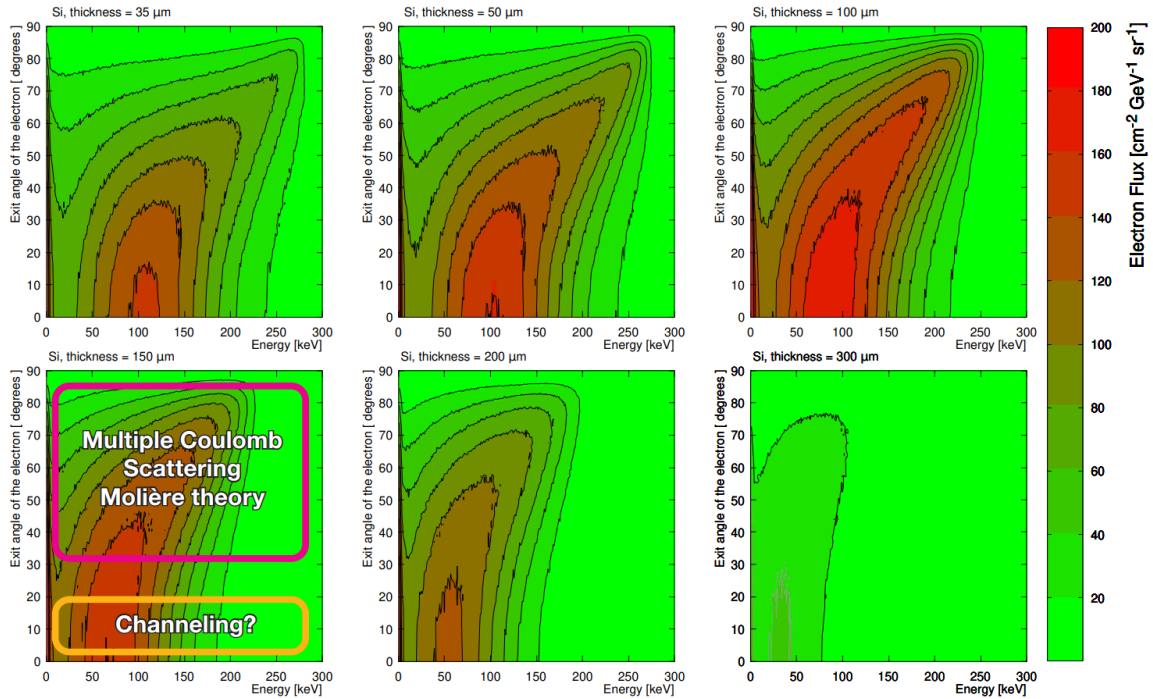


Figure 6: Distribution of the backscattered electrons exiting from the VACNT layer as a function of energy and exit angle for silicon sensor with different thicknesses.

4. Conclusions

VACNTs are a very interesting material that could be used in our detectors to reduce the material budget, granting mechanical stability and, optimizing thermal and electrical conductivity at the same time. The usage of VACNT would not only be limited to MAPS detectors but could also be applied to hybrid-pixel detectors. Accurate modelling of the interaction in the VACNTs (with adequate experimental verification) is required to quantify their potential effect on the DQE of a detector.

References

- [1] <https://project-allpix-squared.web.cern.ch/project-allpix-squared/>
- [2] G. Cavoto *et al.*, *Carbon nanotubes as anisotropic target for dark matter*, Journal of Physics: Conference Series, Volume 1468 doi: 10.1088/1742-6596/1468/1/012232
- [3] G. D’Acunto *et al.*, *Channelling and induced defects at ion-bombarded aligned multiwall carbon nanotubes*, Carbon 139 (2018) 768, doi: 10.1016/j.carbon.2018.07.032
- [4] R. Engel-Hebert *et al.*, *Growth of carbon nanotubes on GaAs*, doi: 10.1016/j.matlet.2007.02.063
- [5] G. Battistoni *et al.*, *Overview of the FLUKA code*, Annuals of Nuclear Energy 82, 10-18 (2015), doi: 10.1016/j.anucene.2014.11.007

- [6] C. Ahdida *et al.*, *New Capabilities of the FLUKA Multi-Purpose Code*, *Frontiers in Physics* 9, 788253 (2022), doi: [10.3389/fphy.2021.788253](https://doi.org/10.3389/fphy.2021.788253)
- [7] J. Allison *et al.*, *Recent developments in Geant4*, doi: [10.1016/j.nima.2016.06.125](https://doi.org/10.1016/j.nima.2016.06.125)
- [8] I. Kyriakou *et al.*, *Monte Carlo study of electron-beam penetration and backscattering in multi-walled carbon nanotube materials*, doi: [10.1063/1.4792231](https://doi.org/10.1063/1.4792231)
- [9] A. Nojeh, *Carbon Nanotube Electron Sources: From Electron Beams to Energy Conversion and Optophotonics*, *ISRN Nanomaterials Volume 2014*, Article ID 879827, doi: [10.1155/2014/879827](https://doi.org/10.1155/2014/879827)
- [10] F. Salvat *et al.*, *Penelope-2006: A code system for Monte Carlo simulation of electron and photon transport*, *OECD/NEA Data Bank*. (2006), ISBN 92-64-02301-1
- [11] V.-T. Rangel-Kuoppa *et al.*, *Towards GaAs Thin-Film Tracking Detectors*, doi: [10.1088/1748-0221/16/09/P09012](https://doi.org/10.1088/1748-0221/16/09/P09012)
- [12] C.C. Yap *et al.*, *Carbon nanotube bumps for the flip chip packaging system*, *Nanoscale Research Letters* 2012, 7:105, doi: [10.1186/1556-276X-7-105](https://doi.org/10.1186/1556-276X-7-105)